Int. J. Bio-Inorg. Hybr. Nanomater., 4(4): 233-242, Winter 2015

Hydrolysis of semi mustard (S.M) by $MnCo_2O_4$ ($MnO\text{-}Co_2O_3$) nanocomposite as a binary oxide catalyst: kinetics reactions study

M. Sadeghi[1]; S. Yekta[2]; E. Babanezhad[3]*

[1] *Young Researchers and Elite Club, Ahvaz Branch, Islamic Azad University, Ahvaz, Iran*
[2] *Department of Chemistry, Faculty of Basic Sciences, Islamic Azad University, Qaemshahr Branch, Qaemshahr, Iran*
[3] *Department of Applied Chemistry, Faculty of Pharmaceutical Chemistry, Pharmaceutical Sciences Branch, Islamic Azad University, Tehran, Iran*

Received: 23 September 2015; Accepted: 25 November 2015

ABSTRACT: $MnCo_2O_4$ ($MnO\text{-}Co_2O_3$) nanocomposite as a binary oxide has been successfully prepared by precipitation method using cobalt nitrate and manganese nitrate as the precursors and then characterized by scanning electron microscopy-energy dispersive micro-analysis (SEM-EDX) and X-ray diffraction (XRD) techniques. In this work, we report the hydrolysis kinetics reactions of semi mustard (chloroethyl ethyl sulfide (CEES)/S.M), a mimic of bis (chloroethyl) sulfide (i.e. sulfur mustard) that were carried out on the surface of $MnCo_2O_4$ nanocomposite as a destructive sorbent catalyst and were performed using GC-FID and GC-MS instruments. The effect of different parameters including solvent type and reaction time on the reaction efficiency were investigated. GC-FID analysis results emphasized that the maximum hydrolysis of CEES was related to *n*-hexane nonpolar solvent after the elapse of the reaction (12 h) at room temperature (25±1°C) with a 95% yield. On the other hand, minimum hydrolysis was reported for methanol polar solvent under similar conditions. The rate constant and half-life ($t_{1/2}$) have been calculated 6.91×10^{-6} s^{-1} and 6.98×10^{-5} s^{-1}, and 105 s and 9.9×10^{3} s for methanol and *n*-hexane solvents, respectively. Also, Data explore the role of the hydrolysis product, i.e. hydroxyl ethyl ethyl sulfide (HEES) in the reaction of CEES with $MnCo_2O_4$ nanocomposite and GC-MS analysis was applied to identify and quantify semi mustard destruction product.

Keywords: *Binary oxide; Chloroethyl ethyl sulfide (CEES); Hydrolysis; Hydroxyl ethyl ethyl sulfide (HEES); Kinetic; $MnCo_2O_4$ nanocomposite*

1. INTRODUCTION

With the arrival of the new century, the fading use of chemical warfare agents (CWAs) as threats to the worldwide community has emerged again which posed renewed concerns in the very recent years. While vexing reports from Middle East and Syria during the last year have shown the crisis of CWAs such as sulfur mustard used by terrorist organizations as they are cheap and easy to manufacture, devastating effects manifested in case of military actions, large worldwide stock of ammunition and certainly on the specter of terrorist attack (Ahmed, *et al.*, 2012, Wellert, *et al.*, 2008) have added research interests for the catalytic decontamination of CWA upon identifying new highly

(*) Corresponding Author - e-mail: meysamsadeghi45@yahoo.com

reactive decontaminants. Over time, adsorption of the toxic agents and subsequently degradation and neutralization strategies have been emerged in the spotlight of researchers, necessarily for research in countering terrorism and military defense units. One of the most known CWA is sulfur mustard (bis(chloroethyl) sulfide) with the molecular formula of $(ClCH_2CH_2)_2S$, commonly abbreviated as H for munition grade and D for distilled). Less toxic analogues (agent simulants) such as semi mustard (S.M) or chloroethyl ethyl sulfide (CEES) with physicochemical properties similar to those of the agent could be generally subjected for the research studies due to extreme toxicity of HD. One of the main challenges for the decontamination of HD and its analogues is their permanency which makes them extremely hazardous. When a person exposed with these compounds blistering of the skin and mucous membranes is very common. Hence, they are so-called vesicants or blistering agents (Munro, *et al.*, 1999). A lot of attentions have been paid toward improving the reactivity of metal oxides as solid adsorptive catalysts to replace the traditional liquid decontamination of HD and its simulants (Joseph, *et al.*, 1999, Ozgr, *et al.*, 2004, Ohtomo and Tsukazaki 2005, Schmidt, *et al.*, 2003, Wang, *et al.*, 2009). The investigations have proved metal oxide nanostructures as potential adsorbents for the catalytic decontamination of HD and its simulants (Prasad 2010, Prasad 2009, Sadeghi, *et al.*, 2013, Sadeghi and Husseini 2012, Sadeghi and Husseini 2013).

Recent investigations have explored the promising decomposition applications of the nano-sized metal oxides such as AP-MgO, AP-CuO, AP-Fe_2O_3 and AP-Al_2O_3 (Mirzaei, *et al.*, 2006, Luisetto, *et al.*, 2008, Rios, *et al.*, 2010, Shinde, *et al.*, 2006, Ahmed, *et al.*, 2008, Sun, *et al.*, 2009). In recent years, cobalt oxide (Co_3O_4) and manganese-cobalt oxide ($MnCo_2O_4$) spinel nanocomposite (Rios, *et al.*, 2010) has been extensively studied owing to their potential uses in many fields including solar energy cells as photoelectric energy conversion materials (Wagner, *et al.*, 1999, Wagner, *et al.*, 2000). A variety of methods has been reported for the preparation of Co_3O_4 and $MnCo_2O_4$ nanocomposite including chemical spray pyrolysis (Shinde, *et al.*, 2006), chemical vapor deposition (CVD) (Ahmed, *et al.*, 2008), micro-emulsion synthesis (Sun, *et al.*, 2009), solvo-thermal synthesis (Rumplecker, *et al.*, 2007), hydrothermal method (Yang, et al., 2004), mechano-chemical method (Tao, *et al.*, 2004) and chemical combustion synthesis (Rusu, *et al.*, 2000). Nevertheless, nearly all of these methods need specific instrumentation and harsh conditions. Martin-de-Vidales, *et al.*, 1993, prepared Co_3O_4 nanoparticles and $MnCo_2O_4$ nanocomposite by sol-gel method. They reported that using this route, size, and morphology and crystal structure of the products could be easily controlled. In the present study, the characterization of $MnCo_2O_4$ (MnO-Co_2O_3) nanocomposite as a binary oxide (manganese-cobalt oxide) synthesized by precipitation method at 400°C is investigated. $MnCo_2O_4$ nanocomposite were then evaluated as solid catalyst for the hydrolysis of semi mustard or chloroethyl ethyl sulfide (CEES) on their surface $MnCo_2O_4$ nanocomposite at room temperature (RT(25±1°C)) in different solvents such as methanol and *n*-hexane and kinetics of reactions were studied using GC-FID.

EXPERIMENTAL DETAILS

Materials and reagents

$Co(NO_3)_2.6H_2O$, $Mn(NO_3)_2.4H_2O$, KOH, toluene, methanol and *n*-hexane were purchased from Merck (Merck, Darmstadt, Germany). Chloroethyl ethyl sulfide (CEES) was obtained commercially from Sigma-Aldrich Co. (USA). All the chemicals were used as received and were of chemical grade.

Instrumentation

The morphology and approximate size of the prepared catalysts were studied via SEM images using a scanning electron microscope coupled with energy dispersive X-ray spectrometer (SEM-EDX, HITACHI S-300N). The powder X-ray diffraction pattern (XRD, Philips PW 1800) study was carried out on an X-ray diffractometer using CuKα radiation (30 mA and 20 kV and λ= 1.54056 Å). The analyses were conducted at 2° min-1 in the range of 2θ= 10-80°. A Varian Star 3400CX series gas chromatograph equipped with flame ionization detector (FID) and an OV-101CWHP 80/100 silica capillary column (30 m×0.25 mm inner diameter (i.d.), 0.25 μm film thickness) was used

to monitor the hydrolysis reactions of the semi mustard, CEES. The extracted products were analyzed by a HP-Agilent gas chromatograph-mass spectrometer equipped with a fused-silica capillary column (DB 1701, 30 m×0.25 mm inner diameter (i.d.), 0.25 μm film thickness). The GC conditions used were as follows: the column temperature was initially hold at 60°C for 6 min and programmed at 20°C min^{-1} to 200°C to reach the final temperature which was then held for 13 min. The injector, MS quad and source temperatures were fixed at 60°C, 200°C and 230°C, respectively. Helium (99.999% purity) was selected as the carrier gas with the flow rate of 1 $mL.min^{-1}$.

Preparation of Co_3O_4 and $MnCo_2O_4$

Prior to the reaction, Co_3O_4 nanoparticles and $MnCo_2O_4$ nanocomposite were synthesized by precipitation method as previously reported (Martin-de-Vidales, *et al.*, 1993). For this purpose, 2 g of $Co(NO_3)_2.6H_2O$ as the source of Co_2^+ ions was dissolved in 100 mL of deionized water. Then, 100 mL of 3.2 M KOH aqueous solution was added drop-wise to the precursor solution. Pink precipitate appeared immediately which was oxidized $Co(OH)_3$ easily by air and low heat or by weak oxidizing agents. As a result, a dark brown precipitate was produced which was separated and washed with deionized water, then dried in an oven at 60°C for 30 min. Reactions of $Co(OH)_3$ production are as follows (1-3):

$$Co(NO_3)_2.6H_2O+KOH \rightarrow Co(OH)NO_3+ KNO_3 \quad (1)$$

$$Co(OH)NO_3 + KOH \rightarrow Co(OH)_2 + KNO_3 \quad (2)$$

$$4\ Co(OH)_2+O_2 + 2H_2O \rightarrow 4\ Co(OH)_3 \quad (3)$$

For the preparation of cobaltic-cobaltous oxide (Co_3O_4), the dark brown cobaltic hydroxide was calcined at 400°C for 5 h.

On the other hand, to synthesize the $MnCo_2O_4$ nanocomposite, 1 g of $Mn(NO_3)_2.4H_2O$ and 2 g of $Co(NO_3)_2.6H_2O$ were dissolved in 100 mL of deionized water. While stirring vigorously, KOH was added until a homogeneous mixture was observed which then was dried at 60°C for 30 min. Finally, the calcination of this powder was also carried out at 400°C for 5 h.

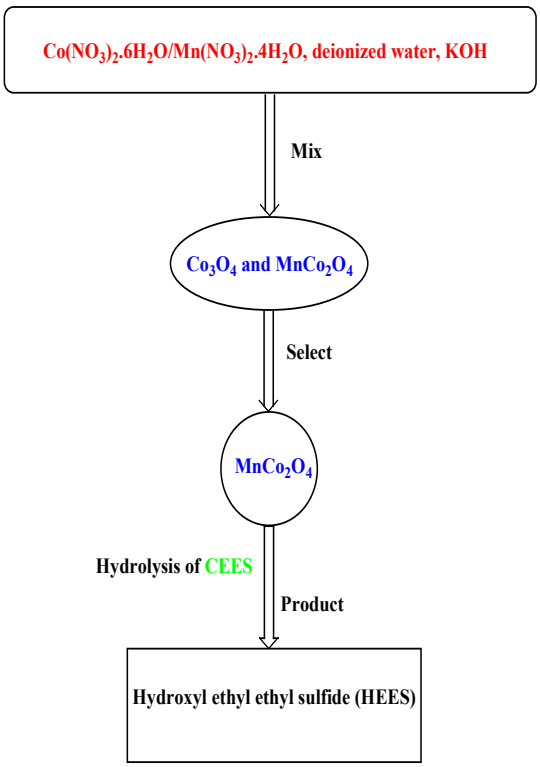

Scheme 1: The diagram for the synthesis of $MnCo_2O_4$ nanocomposite and its hydrolysis product with semi mustard (CEES).

Hydrolysis procedure of the CEES by $MnCo_2O_4$ nanocomposite as binary oxide catalyst

The CEES molecule was hydrolyzed on the surface of $MnCo_2O_4$ nanocomposite according to the following procedure: First, 15 μL of toluene as internal standard and 15 μL of a 5:1 (v/v) ratio of CEES/H_2O were added to 15 mL of each solvent (methanol and *n*-hexane) representing the optimizing work solutions, in a 20 mL Erlenmeyer flask which was sealed to prevent the vaporization of the solvents. All samples were vortexes for 1 min to give blank samples. 0.3 g of $MnCo_2O_4$ nanocomposite powder was then added to above solutions. No efforts were made to control ambient light or humidity. To achieve a perfect adsorption and a complete reaction between $MnCo_2O_4$ nanocomposite and semi mustard, all samples were shaken at periodic intervals until 12 h on a wrist-action shaker to study kinetics hydrolysis. After agitation of solution samples, they left until the precipitation process fulfilled. Finally, 10 μL of upper solution of each samples brought out via a micro-syringe and injected to columns of GC-FID and GC-MS instruments for studying the kinetics of hydrolysis of CEES. In scheme 1,

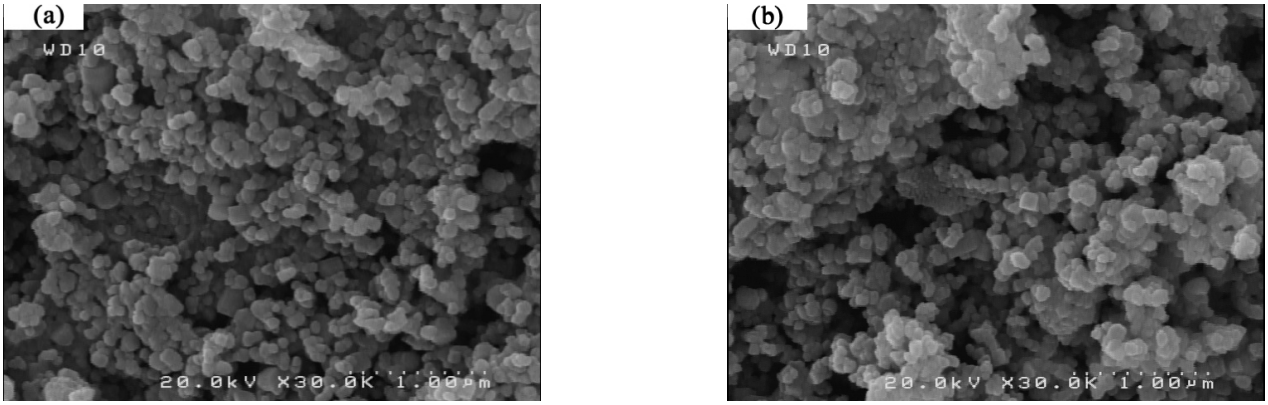

Fig. 1: SEM images of: (a) Co_3O_4 nanoparticles and (b) $MnCo_2O_4$ nanocomposite.

the diagram for the synthesis of $MnCo_2O_4$ nanocomposite and its hydrolysis product with CEES is shown.

RESULT AND DISCUSSION

SEM analysis

The SEM images of cobalt oxide (Co_3O_4) nanoparticles and manganese-cobalt oxide spinel ($MnCo_2O_4$) nanocomposite for the investigation of the morphology and structure at 400°C are shown in Figs. 1a and 1b, respectively. Analyzing the morphology aspect of nanocomposite indicates that the sample consists of quasi-cubic particles. The results have also emphasized that both two catalysts have nano-sized particles (less than 100 nm).

EDX analysis

The energy dispersive X-ray (EDX) microanalysis was performed to confirm the presence of cobalt, manganese and oxygen elements in the catalyst samples. As indicated in Figs. 2a and 2b, there was no unidentified peak observed in the EDX spectra (only C element has been revealed which was corresponded to adsorbed atmospheric CO_2). This fact clearly confirms the prepared purity and composition of Co_3O_4 nanoparticles and $MnCo_2O_4$ nanocomposite.

X-ray diffraction (XRD) patterns

In Fig. 3, the structures of the nano-structured samples have been assayed by X-ray diffraction patterns of each sample at 400°C as shown. The crystalline size was determined from full width at half maximum (FWHM) parameter with the most intense peak obtained in XRD patterns. The average particle size of Co_3O_4 nanoparticles and $MnCo_2O_4$ nanocomposite were calculated from line broadening of the peak at 2θ= 10-80° using Debye-Scherrer formula (4) (Radwan, *et al.*, 2007):

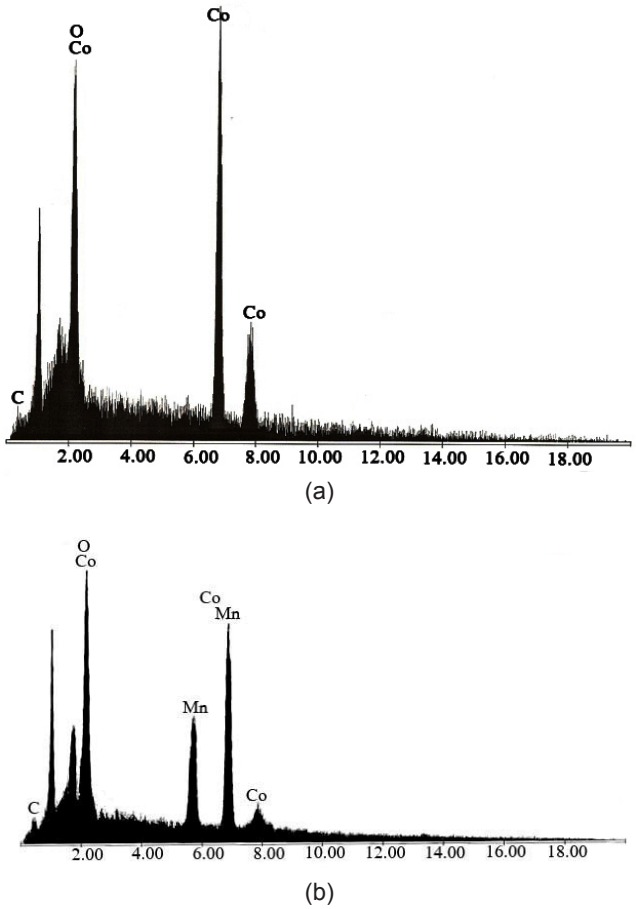

Fig. 2: EDX analysis of: (a) Co_3O_4 nanoparticles and (b) $MnCo_2O_4$ nanocomposite.

$$d = \frac{0.94\lambda}{\beta \cos\theta} \quad (4)$$

Where d is the crystalline size, λ is the wavelength of X-ray Cu Kα source (λ= 1.54056 Å), β is the full width at half maximum (FWHM) of the most predominant peak at 100% intensity and θ is Bragg diffraction angle at which the peak is recorded. There were no characteristic peaks corresponded to of impurity were found, confirming that high-purity products be obtained. In two of the XRD patterns, seven peaks were revealed at approximately 2θ= 23.11°, 28.45°, 37.36°, 45.55°, 55.52°, 58.68°, and 63.74°, which correspond to the Bragg's reflection plane (111), (220), (311), (400), (422), (511) and (440) for cobalt oxide and four peaks at 2θ = 16.36°, 33.38°, 43.19° and 76.73°, related to the Bragg's reflection plane (110), (310), (300) and (421) for manganese oxide (Mn-O) nanoparticles, respectively. Using this formula, the smaller average particle sizes were estimated to be 27.29 nm and 22.19 nm for Co_3O_4 nanoparticles with (JCPDS 74-2120) and $MnCo_2O_4$ nanocomposite with (JCPDS 23-1237), respectively. The β of the XRD peaks may also contain contributions from lattice microstrain. The average microstrain (ε) of the Co_3O_4 nanoparticles and $MnCo_2O_4$ nanocomposite were calculated using the Stocks-Wlison equation (5) (Shakur 2011):

$$\varepsilon = \beta / 4\tan\theta \quad (5)$$

Using this equation, the average microstrain was calculated about 0.25 and 0.31, respectively. The sizes obtained from XRD measurement are consistent with the results from the SEM study.

Kinetics reaction study and GC-FID analysis

The hydrolysis Kinetics reaction of semi mustard (CEES) on the $MnCo_2O_4$ nanocomposite surface was evaluated at room temperature (RT, 25±1°C) and those progresses were studied by GC-FID analysis. Effects of influencing parameters including polarity of the media and the choice of solvent type and reaction time

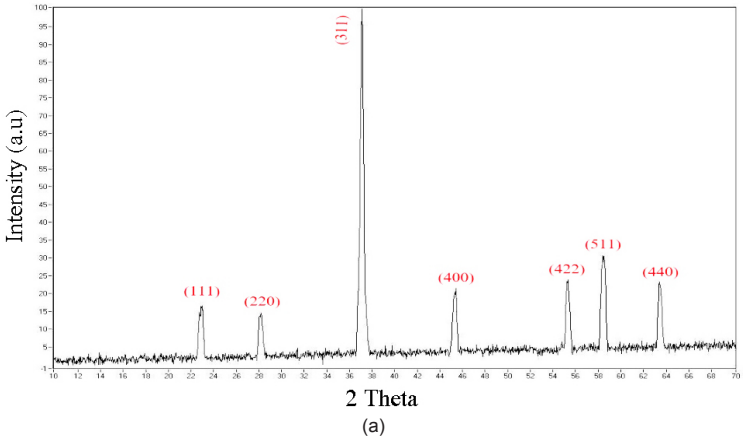

Fig. 3: XRD patterns of: (a) Co_3O_4 nanoparticles and (b) $MnCo_2O_4$ nanocomposite.

have been explored through utilizing methanol and *n*-hexane as the polar and nonpolar solvents and a 2 to 12 h range as shaking time of the reaction, respectively. The GC-FID chromatograms, the area under curve (AUC) data results under above parameters have been summarized in Figs. 4-7. The parameters of a, b, c, d, e, f and g are related to time intervals of 0, 2, 4, 6, 8, 10 and 12 h, respectively (Figs. 4 and 5). It can be showed from the GC-FID chromatograms that CEES eluted at about 10.3 min. To calculate the amounts of hydrolysis reaction, the integrated AUC data of two samples, CEES and toluene as internal standard for all variables were measured and its ratio (integrated AUC of CEES/integrated AUC of toluene) was determined. The results are shown in Fig. 6. Results have illustrated that with decrease in polarity along with increasing the time, the intensity of the AUC data of CEES were declined respect to that of toluene and higher amounts of this molecule were hydrolyzed which are illustrated by new peak at retention times of 14.4 min referring to the product respectively. Eventually, the experiments clearly noted that the perfect hydrolysis occurred in *n*-hexane after 12 h. Generally base sites present on the surface of $MnCo_2O_4$ nanocomposite whether the surface is acidic. Not withstanding the transition state must be involved in the polar reaction, polar solvent hinders the reaction's progress. It could be construed from GC-FID analysis that polar solvent can cover the reactive sites presented on the surface of $MnCo_2O_4$ nanocomposite including Lewis sites. Although the presence of high polarity poisons the adsorption sites, directly adding slight amount of H_2O into the surface of $MnCo_2O_4$ nanocomposite would activate the acid sites and accelerate the hydrolysis of CEES. Positive water effect was also observed for the hydrolysis of semi mustard in literature (Ahmed, *et al.*, 2008). In particular, despite of a large number of strong Lewis acid sites originated from high surface area $MnCo_2O_4$ nanocomposite, the blocking of these adsorptive sites would hinder the coordination of CEES. Since methanol is considered as such a strong hindrance to the reaction, this tends to lend further support to the idea that methanol simply blocks access to the surface of the catalyst. Thus, further reactions were investigated in *n*-hexane solvent. Surveying the reaction between $MnCo_2O_4$ nanocomposite and CEES through GC analysis showed that if one allows for enough time, high destructive catalysis would readily occur. Surveying the reaction between $MnCo_2O_4$ nanocomposite and CEES through GC-FID analysis showed that if one allows for enough time, maximum destructive catalysis would readily occur. In fact, 95% of CEES was hydrolyzed by this catalyst after 12 h. Diagrams illustrating the amount of hydrolyzed and -Ln(a-x)/a versus time in Fig. 7 point out to the fact that reaction times induce a kinetic effect in which the number and vicinity of reactive sites with CEES molecules making them adsorb and destruct, access to these sites and their catalytic capacity increase with time. In Fig. 7, the parameter (a) refers to the state when the amount of CEES is virgin unreacted with $MnCo_2O_4$ nanocomposite and the parameter (x) related to the beginning of CEES reaction with $MnCo_2O_4$ nanocomposite till the end of reaction in which the CEES is hydrolyzed and decontaminated about 95%. Fig.7 has been drawn according to the data which has obtained from Fig. 6. In Fig. 6, decontaminated CEES% was utilized for the calculation of –Ln (a-x)/a versus reaction time which has mentioned in Fig. 7. The linearity in Ln diagrams 7 elucidates that the kinetics of the reaction have a first order steady state behavior. The formula (6) in below is used for calculation of half-life ($t_{1/2}$) of the hydrolysis reaction. In this formula, parameter (k) is defined as diagram slope of –Ln (a-x)/a versus 1/h which equals to rate constant.

$$t_{1/2} = 0.693 / k \quad (6)$$

The average rate constant and reaction half -life using slope of the diagram were measured as 6.91×10^{-6} s^{-1} and 6.98×10^{-5} s^{-1}, and 105 s and 9.9×10^{3} s for methanol and *n*-hexane solvents, respectively.

GC-MS analysis

To understand the hydrolysis product of semi mustard with $MnCo_2O_4$ nanocomposite gas chromatography coupled with mass spectrometry (GC-MS) analysis was used. The mass spectra of semi mustard (chloroethyl ethyl sulfide (CEES)) and hydroxyl ethyl ethyl sulfide (HEES) were shown in Fig. 8. The detector was set to scan a mass range of 28, 43, 61, 75, 91, 109 and 123 m/z and 28, 43, 61, 75, 91 and 106 m/z for CEES

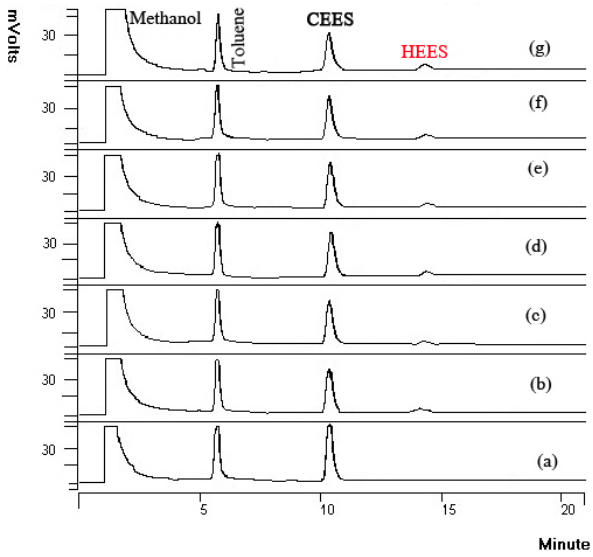

Fig. 4: GC-FID chromatograms for CEES/$MnCo_2O_4$ nanocomposite sample at different times, a) 0, b) 2, c) 4, d) 6, e) 8, f) 10 and g) 12 h, in methanol solvent

and HEES, respectively. This observation emphasizes role of hydrolysis reaction of CEES to HEES.

Mechanism of the hydrolysis procedure

According to the above results, a proposed mechanism of hydrolysis of this reaction will provide in Scheme 2. The mechanism scheme reflecting the reaction steps of the semi mustard adsorption on the $MnCo_2O_4$ nanocomposite along with the formation of hydrolysis product are proposed (Scheme 2) in which the decontamination reactions through cobalt and manganese species (Co^{3+} and Mn^{2+}) species have been reviewed. It is worth-noting that one of the proposed pathways is possible and may proceed simultaneously. In this pathway, adsorption reaction of semi mustard occur through nucleophillic attack of the Bronsted (isolated hydroxyl groups (Co-OH and Mn-OH)) acid sites presented on the $MnCo_2O_4$ of the external surface of the nanocomposite to C-Cl bond of CEES molecule (initially, cyclic sulfonium ion seems to be formed as an intermediate which is in the nonvolatile form of the related compound so that could not be extracted out and detected by GC-FID instrument).

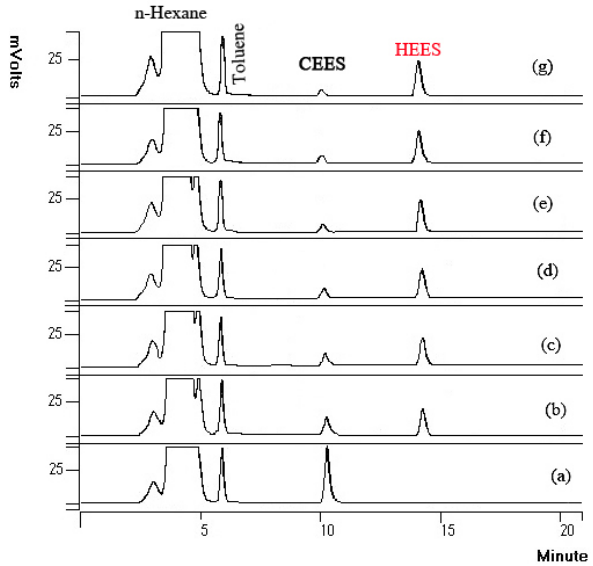

Fig. 5: GC-FID chromatograms for CEES/$MnCo_2O_4$ nanocomposite sample at different times, a) 0, b) 2, c) 4, d) 6, e) 8, f) 10 and g) 12 h, in *n*-hexane solvent.

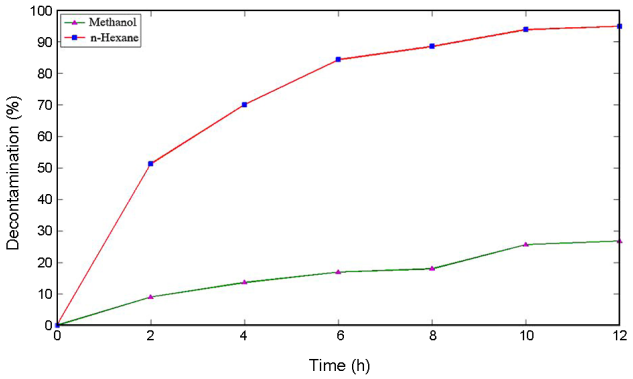

Fig. 6: The curves of decontamination% versus time for CEES/$MnCo_2O_4$ nanocomposite sample in different solvents.

In conclusion, the chlorine atom of CEES will be removed through the dehalogenation reaction. In continuation, in the presence and absence of water molecule, different reactions may proceed and hydrolysis product on the surfaces of Co^{3+} and Mn^{2+} as Lewis acid sites will be illustrated. The hydrolysis reaction of CEES has a single destruction product, namely hy-

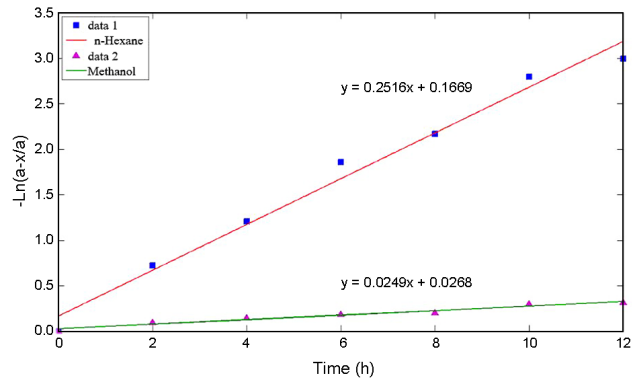

Fig. 7: The diagrams of –Ln (a-x)/a versus time for CEES/$MnCo_2O_4$ nanocomposite sample in different solvents.

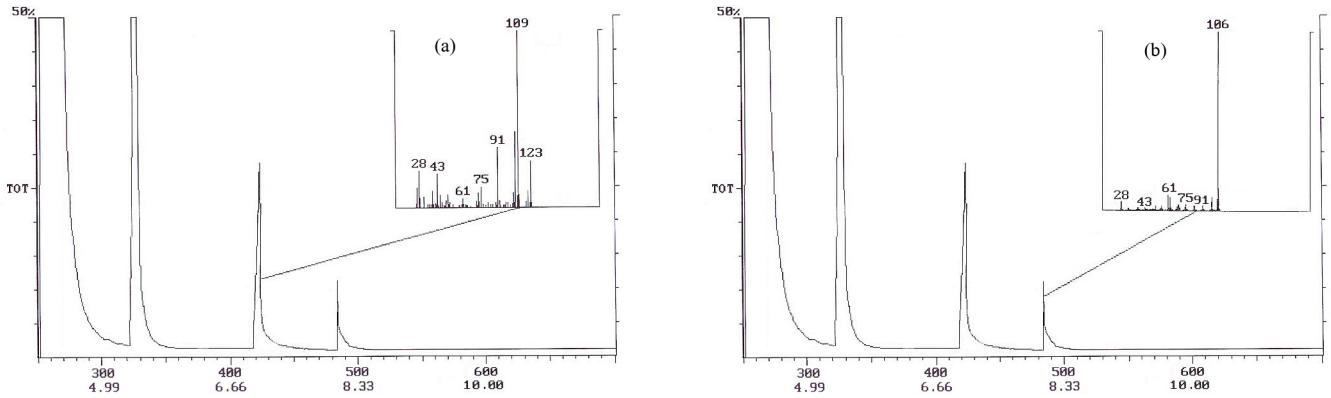

Fig. 8: GC-MS of CEES and hydrolysis product of $MnCo_2O_4$ nanocomposite reaction with CEES: a) chloroethyl ethyl sulfide and b) hydroxyl ethyl ethyl sulfide.

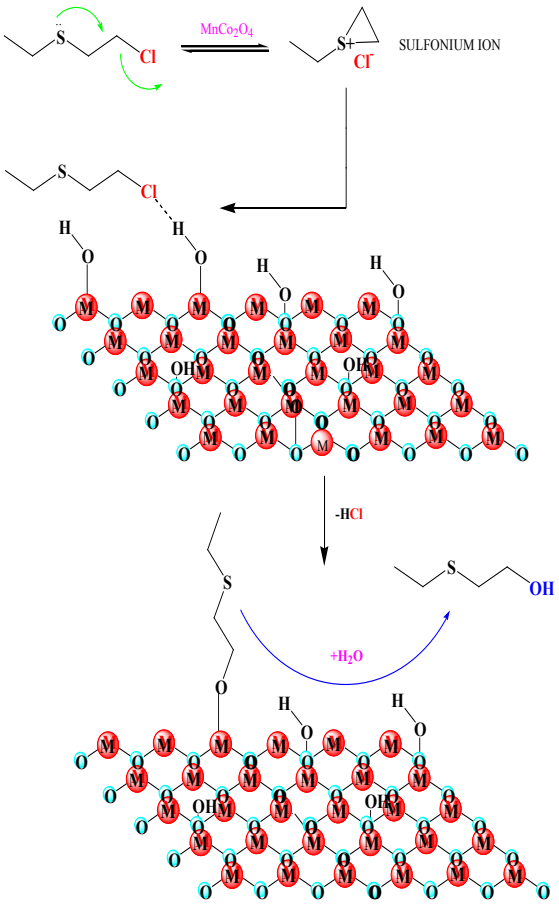

Scheme 2: Reaction mechanism pathway for the hydrolysis of CEES on the surface of the MCo_2O_4 nanocomposite catalyst (M=Mn or/and Co).

droxyl ethyl ethyl sulfide (HEES). Similar results for the hydrolysis and destruction product were also observed by other researchers in several studies (Prasad 2010; Sadeghi and Yekta 2014, Mahato, *et al.*, 2010, Kanyi, *et al.*, 2009).

COCLUSIONS

In summary, $MnCo_2O_4$ nanocomposite has been synthesized by the hydrothermal method. The synthesized samples were characterized via SEM-EDX and XRD techniques. The unique property of synthesized $MnCo_2O_4$ nanocomposite catalyst for the hydrolysis of CEES was investigated by consideration of different parameters namely solvent type and reaction time at room temperature. Based on the observations obtained by GC-FID analysis, the utilized adsorbent catalyst possesses such a high performance and potential for the hydrolysis of the mentioned CEES. The obtained results revealed that the above semi mustard was hydrolyzed on the surface of $MnCo_2O_4$ nanocomposite in *n*-hexane solvent after 12 h at room temperature with a 95% yield and followed via first order steady state behavior. On the other hand, GC-MS analysis has provided valuable information about the single hydrolysis reaction product of semi mustard, namely hydroxyl ethyl ethyl sulfide (HEES).

ACKNOWLEDGMENT

The authors gratefully acknowledge the financial supports of Young Researchers and Elite Club, Ahvaz Branch, Islamic Azad University, Ahvaz, Iran

REFERENCES

Ahmed, F.; Gutch, P.K.; Ganesan, K.; Vijayaragha-

van, R.; (2012). N,N′-dichloro-bis[2,4,6-trichlorophenyl]urea (CC2) and Suspending Agents Used for the Preparation of Decontamination Formulation Against Chemical Warfare Agents A study of Compatibility by Thermoanalytical Techniques. J. Therm. Anal. Calorim., 107 (1): 141-147.

Ahmed, J.; Ahmad, T.; Ramanujachary, K.V.; Lofland, S.E.; Ganguli, A.K.; (2008). Development of a Microemulsion-Based Process for Synthesis of Cobalt (Co) and Cobalt Oxide (Co_3O_4) Nanoparticles from Submicrometer Rods of Cobalt Oxalate. J. Colloid. Interf. Sci., 321(2): 434–441.

Joseph, M.; Tabata, H.; Kawai, T.; (1999). p-Type Electrical Conduction in ZnO Thin Films by Ga and N Codoping. J. Appl. Phys., 38 (2): 1205-1207.

Kanyi, C.W.; Doetschman, D.C.; Schulte, J.T.; (2009). Nucleophilic Chemistry of X-type Faujasite Zeolites with 2-Chloroethyl Ethyl Sulfide (CEES), a Simulant of Common Mustard Gas. Micropor. Mesopor. Mater., 124 (1-3): 232–235.

Luisetto, I.; Pepe, F.; Bemporad, E.; (2008). Preparation and Characterization of Nano Cobalt Oxide. J. Nanopart. Res., 10 (1): 59-67.

Mahato, T.H.; Prasad, G.K.; Singh, B.; Batra, K.; Ganesan K.; (2010). Mesoporous Manganese Oxide Nanobelts for Decontamination of Sarin, Sulphur Mustard and Chloro Ethyl Ethyl Sulphide. Micropor. Mesopor. Mater., 132(1-2): 15-21.

Martin-de-Vidales, J.L.; O Garcfa-Martinez.; Vila E.; Rojas R.M.; Torralvo M.J.; (1993). Low Temperature Preparation of Manganese Cobaltite Spinels [MnxCo3−xO4 (0≤x≤ 1)]. Mat. Res. Bull., 28 (11): 1135-1143.

Mirzaei, A.A; Feyzi, M.; Habibpour, R.; (2006). Effect of Preparation Conditions on the Catalytic Performance of Cobalt Manganese Oxide Catalysts for Conversion of Synthesis Gas to Light Olefins. Appl. Catal. A., 306 (1): 98-107.

Munro, N.B.; Talmage, S.S.; Griffin, G.D.; Waters, L.C; Watson, A.P.; King, J.F.; Hauschild, V.; (1999). The Sources, Fate, and Toxicity of Chemical Warfare Agent Degradation Products. Environ. Health. Perspec., 107(12): 933-974.

Ohtomo, A.; Tsukazaki, A.; (2005). Pulsed Laser Deposition of Thin Films and Superlattices Based on ZnO Semicond. Sci. Technol., 20 (4): 1-12.

Ozgr, U.; Alivov, Y.I.; Liu, C.; Teke, A.; Reshchikov, M.A.; Avrutin, V.; Cho, S.J.; Mork, H.; (2004). A Comprehensive Review of ZnO Materials and Devices. J. Appl. Phys., 98(4): 041301.

Prasad, G.K.; (2010). Decontamination of 2 chloro ethyl phenyl sulphide using mixed metal oxide nanocrystals. J. sci. Ind. Res., 69 (11): 835-840.

Prasad G.K.; (2009). Silver Ion Exchanged Titania Nanotubes for Decontamination of 2-Chloro Ethyl Phenyl Sulphide and Dimethyl Methyl Mhosphonate. J. Sci. Ind. Res., 68 (05): 379-384.

Radwan, N.R.E.; El-Shallb, M.S.; Hassan, H.M.A.; (2007). Synthesis and Characterization of Nanoparticle Co_3O_4, CuO and NiO Catalysts Prepared by Physical and Chemical Methods to Minimize Air Pollution. Appl. Catal. A., 331 (1): 8–18.

Rios, E.; Lara, P.; Serafini, D.; Restovic, A.; Gautier, J.; (2010). Synthesis and Characterization of Manganese- Cobalt Solid Solutions Prepared at Low Temperature. J. Chil. Chem. Soc., 55(2): 261-265.

Rumplecker, A.; Kleitz, F.; Salabas, E.L.; Schüth, F.; (2007). Hard Templating Pathways for the Synthesis of Nanostructured Porous Co_3O_4. Chem. Mater., 19 (3): 485–496.

Rusu, C.N.; Yates, J.T. Jr.; (2000). Adsorption and Decomposition of Dimethyl Methylphosphonate on TiO2. J. Phys. Chem. B, 104 (51): 12292–12298.

Sadeghi, M.; Husseini, M.; Tafi, H.; (2013). Synthesis and Characterization of $ZnCaO_2$ Nanocomposite Catalyst and the Evaluation of its Adsorption/Destruction Reactions with 2-CEES and DMMP. Int. J. Bio-Inorg. Hybd. Nanomat., 2(1): 281-293.

Sadeghi, M.; Husseini, M.; (2012). Nucleophilic Chemistry of the Synthesized Magnesium Oxide (Magnesia) Nanoparticles via Microwave@sol-gel Process for Removal of Sulfurous Pollutant. Int. J. Bio-Inorg. Hybd. Nanomat., 1(3): 175-182.

Sadeghi, M.; Husseini, M.; (2013). A Novel Method for the Synthesis of CaO Nanoparticle for the Decomposition of Sulfurous Pollutant. J. Appl. Chem. Res., 7 (4): 39-49.

Sadeghi, M.; Yekta, S.; (2014). Significance of Chemical Decomposition of Chloroethyl Phenyl Sulfide (CEPS) using Zinc-Cadmium Oxide (ZnO-CdO)

Nanocomposite. Int. J. Bio-Inorg. Hybd. Nanomat., 3 (4): 219-229.

Schmidt, R.; Rheinlnder, B.; Schubert, M.; Spemann, D.; Butz, T.; Lenzner, J.; Kaidashev, M.E.; Lorenz, M.; Rahm, A.; Semmelhack, H.C.; Grundmann, M.; (2003). High Electron Mobility of Epitaxial ZnO Thin Films on c-plane Sapphire Grown by Multistep Pulsed-laser Deposition. Appl. Phys. Lett., 82 (22): 3901.

Shakur, H.R.; (2011). A Detailed Study of Physical Properties of ZnS Quantum Dots Synthesized by Reverse Micelle Method. Physica E, 44 (3): 641–646.

Shinde, V.R.; Mahadik, S.B.; Gujar, T.P.; Lokhande, C.D.; (2006). Supercapacitive Cobalt Oxide (Co_3O_4) Thin Films by Spray Pyrolysis. Appl. Surf. Sci., 252 (20): 7487–7492.

Sun, L.; Li, H.; Ren, L.; Hu, C.; (2009). Synthesis of Co_3O_4 Nanostructures Using a Solvothermal Approach. Solid state Sci., 11 (1): 108-112.

Tao, L.; Shao-Guang, Y.; Li-Sheng, H.; Ben-Xi, G.; You-Wei, D.; (2004). Formation of Co_3O_4 Nanotubes and the Magnetic Behaviour at Low Temperature. Chinese Phys. Lett., 21(5): 966-969.

Wagner, G.W.; Bartam, P.W.; Koper, O.; Klabunde, K.J.; (1999). Reactions of VX, GD, and HD with Nanosize MgO. J. Phys. Chem. B., 103 (16): 3225–3228.

Wagner, G.W.; Koper, O.B.; LucasE.; Decker, S.; Klabunde, K.J.; (2000). Reactions of VX, GD, and HD with Nanosize CaO: Autocatalytic Dehydrohalogenation of HD. J. Phys. Chem., 104 (21): 5118–5123.

Wang, F.; Liu, B.; Zhang, Z.; Yuan, S.; (2009). Synthesis and Properties of Cd-doped ZnO Nanotubes. Physica E, 41 (5): 879-882.

Wellert, S.; Imhof, H.; Dolle, M.; Altmann, H.J.; Richardt, A.; Hellweg, T.; (2008). Decontamination of Chemical Warfare Agents Using Perchloroethylene-Marlowet IHF-H2O-based Microemulsions: Wetting and Extraction Properties on Realistic Surfaces. Colloid. Polym. Sci., 286 (4): 417-426.

Yang, H.; Hu, Y.; Zhang, X.; Qiu, G.; (2004). Echanochemical Synthesis of Cobalt Oxide Nanoparticles. Mate. Lett., 58 (3-4): 387–389.

AUTHOR (S) BIOSKETCHES

Meysam Sadeghi, M.Sc., Young Researchers and Elite Club, Ahvaz Branch, Islamic Azad University, Ahvaz, Iran, *E-mail: meysamsadeghi45@yahoo.com*

Sina Yekta, M.Sc., Department of Chemistry, Faculty of Basic Sciences, Islamic Azad University, Qaemshahr Branch, Qaemshahr, Iran

Esmaeil Babanezhad, Ph.D., Department of Applied Chemistry, Faculty of Pharmaceutical Chemistry, Pharmaceutical Sciences Branch, Islamic Azad University, Tehran, Iran